Mon. Not. R. Astron. Soc. **000**, 000–000 (0000) Printed 2 February 2008 (MN LaTeX style file v2.2)

On the origin of the C IV Baldwin effect in AGN

Alexei Baskin⋆ & Ari Laor⋆

Physics Department, Technion, Haifa 32000, Israel

arXiv:astro-ph/0403365v1 16 Mar 2004

2 February 2008

ABSTRACT

The origin of the luminosity dependence of the equivalent width (EW) of broad emission lines in AGN (the Baldwin effect) is not firmly established yet. We explore this question for the broad C IV λ1549 line using the Boroson & Green sample of the 87 $z \leq 0.5$ Bright Quasar Survey (BQS) quasars. Useful UV spectra of the C IV region are available for 81 of the objects, which are used to explore the dependence of the C IV EW on various emission properties. We confirm earlier results on the strong correlations of the C IV EW with some of the emission parameters which define the Boroson & Green Eigenvector 1, and with the optical to X-ray slope α_{ox}. In addition, we find a strong correlation of the C IV EW with the relative accretion rate, $L/L_{\rm Edd}$. Since $L/L_{\rm Edd}$ drives some of the Eigenvector 1 correlations, it may be the primary physical parameter which drives the Baldwin effect for C IV.

Key words: galaxies: active – quasars: emission lines – quasars: general – ultraviolet: galaxies.

1 INTRODUCTION

The inverse correlation of the broad emission line equivalent width (EW) with luminosity in AGN, discovered by Baldwin (1977) for the C IV λ1549 line, was intensively explored over the past 20 years (see a comprehensive review by Osmer & Shields 1999; and more recent studies by Wilkes et al. 1999; Green et al. 2001; Croom et al. 2002; Dietrich et al. 2002; Kuraszkiewicz et al. 2002; and Shang et al. 2003). The physical origin for this effect is not clearly established yet, but a plausible explanation is softening of the ionizing continuum shape, and increasing gas metalicity with increasing luminosity (Korista, Baldwin & Ferland 1998). The softening of the ionizing continuum shape with luminosity is supported by: 1. some observed correlations of the emission line strength with the ionizing spectral shape (Green 1998; Wang, Lu & Zhou 1998), 2. predictions of simple accretion disk models for the ionizing spectral shape dependence on luminosity (Netzer, Laor & Gondhalekar 1992), and 3. the dependence of the slope of the Baldwin effect on the ionization potential of the emitting ions (Espey & Andreadis 1999; Green et al. 2001; Dietrich et al. 2002; Kuraszkiewicz et al. 2002). Non isotropic continuum emission (Netzer 1987), and the intrinsic Baldwin effect (Pogge & Peterson 1992; also review in Osmer & Shields 1999, §5) can produce some of the observed scatter in the Baldwin effect for the various lines.

Significant correlations also exist among various optical emission line properties in AGN, including the [O III] and Fe II strength, and the Hβ FWHM, which form part of Eigenvector 1 (EV1) in the comprehensive study of Boroson & Green (1992, hereafter BG92). Boroson, Persson & Oke (1985) speculated that the underlying physical parameter which drives these correlation is the relative accretion rate, $L/L_{\rm Edd}$, a speculation which received strong support through recent observations (see review in Laor 2000). Furthermore, Wills et al. (1999) found that various UV emission properties, including the C IV EW, are correlated with the optical EV1 parameters, which suggests that the C IV EW may also be largely driven by $L/L_{\rm Edd}$. The Baldwin effect may then just be a secondary correlation induced by the tendency of more luminous AGN to have a higher $L/L_{\rm Edd}$. The possible role of $L/L_{\rm Edd}$ in the Baldwin effect was already mentioned by Brotherton & Francis (1999). Later, Wilkes et al. (1999) noted that narrow line AGN are outliers to the Baldwin effect, but the meaning of this result was not interpreted at that time (see §4 here). Most recently Shang et al. (2003) suggested an indirect indication, based on spectral principle component analysis, that $L/L_{\rm Edd}$ may contribute to the scatter in the Baldwin effect.

Recent studies established that reasonably accurate estimates of the black hole mass ($M_{\rm BH}$) can be obtained in AGN based on the continuum luminosity and Hβ FWHM ($M_{\rm BH} \propto L^{1/2}({\rm H}\beta\ {\rm FWHM})^2$, and thus $L/L_{\rm Edd} \propto L^{1/2}({\rm H}\beta\ {\rm FWHM})^{-2}$, e.g. Laor 1998). This opens up the possibility to test directly whether the Baldwin effect is driven by $L/L_{\rm Edd}$, which is the main point of this paper. The data set and measurement procedure are described in §2, the correlation analysis is presented in §3, and the main results are summarized in §4.

⋆ E-mail:alexei@physics.technion.ac.il(AB); laor@physics.technion.ac.il (AL)

2 THE MEASUREMENTS

For the purpose of this analysis we use the BG92 sample which includes the 87 $z < 0.5$ AGN from the Bright Quasars Survey (BQS; Schmidt & Green 1983). This sample extends in luminosity from Seyfert galaxies with $\nu L_\nu = 3.3 \times 10^{43}$ erg s^{-1} (calculated using the continuum fluxes in Neugebauer et al. 1987, assuming $H_0 = 80$ km s^{-1} Mpc^{-1}, $\Omega_0 = 1.0$), to luminous quasars at $\nu L_\nu = 1.4 \times 10^{46}$ erg s^{-1}, where νL_ν is calculated at 3000 Å. This is a complete and well defined sample, selected based on (blue) color and (point like) morphology, independently of the emission line strengths. It is also the most thoroughly explored sample of AGN, with a wealth of high quality data at most wave bands. The EV1 correlations were established by BG92 using this sample, and the ability to obtain reasonably accurate estimates of $M_{\rm BH}$ (and thus $L/L_{\rm Edd}$) was demonstrated for this sample (Laor 1998), thus making it an optimal sample to explore the possible origin of the Baldwin effect.

Archival UV spectra of the C IV region are available for 85 of the 87 BG92 objects. The *HST* archives contain UV spectra of 47 of the objects, which were obtained by the Faint Object Spectrograph (FOS); the UV spectra for the remaining 38 objects with no *HST* spectra were obtained from the *IUE* archives (see Table 1). An average spectrum, weighted by the S/N ratio, was calculated when more than one archival spectrum was available. This averaging should decrease the scatter in the Baldwin effect induced by variability, as demonstrated in the intrinsic Baldwin effect.

Three of the archival spectra (PG 0934+013, PG 1004+130 and PG 1448+273) did not have a sufficient S/N to measure the C IV EW, and in one object (PG 1700+518) C IV is heavily absorbed (e.g. Laor & Brandt 2002), leaving a sample of 81 objects with a measurable C IV EW. The C IV region of PG 0043+039 is also rather heavily absorbed, and its measured C IV EW is probably just a lower limit. The continuum flux uncertainty of the *HST* spectra, which were obtained without the flux density uncertainty from the *HST* archives, was estimated using the average standard deviation of the flux at two windows: 1450 Å - 1470 Å, and 1710 Å - 1730 Å (rest frame)[1]. The rest frame wavelengths were calculated using redshifts determined from the peak of the [O III] λ5007 line (kindly provided by T. Boroson, private communication). The wavelength dependence of the flux density uncertainty (of the *HST* spectra) was assumed to scale with the square root of the ratio of the flux density to continuum flux density. The *IUE* spectra were obtained with the flux density uncertainty from the *IUE* archives.

The spectra were corrected for Galactic reddening using the *E(B−V)* values from Schlegel, Finkbeiner & Davis (1998, as listed in the NASA/IPAC Extragalactic Database), and the reddening law of Seaton (1979). A local power-law continuum was fit to each spectrum between ∼ 1470 Å and ∼ 1620 Å, and the C IV line emission was fit as a sum of three Gaussians, using the procedure described in Laor et al. (1994, §3 and the appendix there). Wavelength regions suspected to be affected by intrinsic or Galactic absorption were excluded from the fit (Laor & Brandt 2002). The purpose of the line fit is not to decompose the line to possible components, but rather to obtain a smooth realization of the line profile, which is likely to yield more accurate values for the line width and EW.

Table 1 presents our measured rest-frame EW of the best-fitting models to the C IV profile, together with the estimated errors. The errors were estimated by repeating the model fits with the power-law continuum displaced upward and downward by 1σ. As expected, the typical errors associated with *IUE* spectra are significantly higher than those of the *HST* spectra. One should note that larger systematic errors could be associated with the placement of the continuum windows. In particular, the presence of very broad weak wings is difficult to detect, although they may have a non-negligible EW. Table 1 also lists νL_ν calculated at 3000 Å for each object, and the estimated $L/L_{\rm Edd}$.

3 THE CORRELATION ANALYSIS

Figure 1 (top panel) presents the Baldwin effect for the 81 BQS quasars measured above. The C IV EW are taken from Table 1, and for the luminosity we use νL_ν at 3000 Å (see §2). To verify that our sample is not biased in any way, we also present in Fig. 1 data from two other studies, 454 Large Bright Quasar Survey objects[2] analyzed by Forster et al. (2001), and 125 pre-COSTAR AGN observations analyzed by Kuraszkiewicz et al. (2002) (which overlap some of our objects). These data are available in public electronic form. The luminosities of these objects were derived from the specified flux densities using the same cosmology assumed for the BQS quasars. The trend and scatter of the Baldwin effect for the BQS quasars appears to be very similar to those displayed by the Forster et al. (2001) and Kuraszkiewicz et al. (2002) samples. The Spearman rank-order correlation coefficient for the BQS Baldwin effect is $r_s = -0.154$. The flattening of the Baldwin relation at low luminosity is clearly seen in Fig. 1 (see discussion in §4.2 of Osmer & Shields 1999). The non-linearity of the Baldwin effect (on log-log scale) suggests that the Spearman rank-order correlation coefficient, which tests for a monotonic relation, is a more suitable statistical test here, compared to the Pearson correlation coefficient, which tests the significance of a linear relation.

Table 2 presents the results of a correlation analysis of the C IV EW reported in Table 1 with all the optical emission line parameters from BG92 (table 2 there), supplemented by α_{ox} from Brandt, Laor & Wills (2000), and $L/L_{\rm Edd}$ and $M_{\rm BH}$ as estimated from the optical luminosity and the Hβ FWHM (equation 3 in Laor 1998). For the sake of brevity we present only the most significant correlations (those where Pr $< 5 \times 10^{-4}$). To explore the effect of the generally lower S/N *IUE* spectra on the strength of the

[1] Lack of data or strong systematic features necessitated the following changes to one or both windows; PG 0003+158: 1465 Å - 1485 Å, PG 1114+445: 1465 Å - 1485 Å, and 1730 Å - 1750 Å; PG 1211+143, PG 1404+226 and PG 1440+356: only the 1710 Å-1730 Å window used; PG 1415+451: used only 1700 Å - 1720 Å; PG 1543+489: 1600 Å - 1620 Å; PG 1612+261: 1470 Å - 1490 Å; PG 2304+042: 1680 Å - 1700 Å.

[2] We have ignored two upper limits in the tabulation of Forster et al. (2001), and several obvious typographical flux errors, in their total list of 488 objects.

Table 1. The C IV EW, νL_ν, and $L/L_{\rm Edd}$ of the 81 BQS quasars.

Object	EW[a]	νL_ν[b]	$L/L_{\rm Edd}$[c]	Object	EW[a]	νL_ν[b]	$L/L_{\rm Edd}$[c]	Object	EW[a]	νL_ν[b]	$L/L_{\rm Edd}$[c]
0003+158	63.5± 4.6	1.877	−0.358	1115+407	25.9± 4.2	0.547	−0.139	1416−121	168.1±40.2	1.337	−0.845
0003+199	60.1± 2.6	0.059	−0.342	1116+215	40.5± 2.9	1.468	−0.139	1425+267	64.8± 10	1.219	−1.280
0007+106	59± 5	0.770	−0.972	1119+120	29± 5	−0.001	−0.462	1426+015	32± 2	0.985	−1.117
0026+129	19.3± 3.9	1.067	0.053	1121+422	41.7± 4.1	0.806	−0.232	1427+480	53.2± 3.7	0.815	−0.344
0043+039	5.4± 3.7	1.485	−0.648	1126−041	30± 7	0.344	−0.434	1435−067	39± 7	1.069	−0.412
0049+171	203± 73	−0.109	−1.437	1149−110	82± 20	−0.006	−0.916	1440+356	30.1± 1.4	0.503	−0.013
0050+124	29.9± 1.5	0.582	0.162	1151+117	26.6± 7.1	0.815	−0.801	1444+407	17.9± 1.1	1.217	−0.122
0052+251	119.0±10.5	1.104	−0.822	1202+281	290.0±31.3	0.590	−1.053	1501+106	64± 1	0.491	−1.172
0157+001	43± 8	0.926	−0.261	1211+143	55.7± 1.8	1.063	0.051	1512+370	84.3± 7.2	1.483	−0.867
0804+761	45± 3	1.233	−0.300	1216+069	64.5± 4.4	1.527	−0.609	1519+226	68± 16	0.647	−0.311
0838+770	50± 10	0.679	−0.493	1226+023	23.0± 0.7	2.045	−0.012	1534+580	79± 6	−0.337	−1.565
0844+349	28± 5	0.461	−0.479	1229+204	48± 3	0.381	−0.804	1535+547	27.6± 1.7	−0.182	−0.373
0921+525	186± 11	−0.415	−0.802	1244+026	17± 4	0.031	0.235	1543+489	25.6± 1.4	1.394	0.369
0923+129	93± 13	−0.250	−0.665	1259+593	15.3± 2.5	1.834	−0.085	1545+210	90.5±10.5	1.421	−0.925
0923+201	28± 6	1.141	−1.134	1302−102	13.1± 1.6	1.850	−0.080	1552+085	47± 16	0.585	0.040
0947+396	55± 4	0.802	−0.909	1307+085	71.2± 8.5	1.071	−0.651	1612+261	94.6±13.9	0.699	−0.395
0953+414	54.9± 5	1.473	−0.196	1309+355	33.5± 5.5	0.915	−0.421	1613+658	54± 3	0.676	−1.457
1001+054	34.9± 4.6	0.806	−0.020	1310−108	78± 16	−0.243	−1.183	1617+175	34± 7	1.030	−0.880
1011−040	25± 5	0.225	−0.146	1322+659	52.6± 3.4	0.847	−0.409	1626+554	45.6± 7.6	0.612	−0.940
1012+008	23± 6	0.931	−0.320	1341+258	62± 20	0.304	−0.756	1704+608	34.8± 5.2	1.606	−0.772
1022+519	38± 11	−0.479	−0.600	1351+236	101± 48	−0.351	−1.748	2112+059	25.5± 3.5	2.131	0.116
1048−090	91± 50	1.524	−0.679	1351+640	43.3± 4.4	0.780	−1.058	2130+099	47± 3	0.619	−0.367
1048+342	46± 17	0.735	−0.687	1352+183	45.1± 6.5	0.851	−0.629	2209+184	54± 21	0.428	−1.353
1049−006	67.0± 8.8	1.540	−0.630	1402+261	30.3± 2.8	1.044	0.018	2214+139	45± 4	0.462	−1.027
1100+772	84.0± 4.9	1.544	−0.749	1404+226	23.3± 3.4	0.126	0.232	2251+113	66.0± 3.5	1.634	−0.363
1103−006	37.2± 9	1.575	−0.737	1411+442	56.9± 18	0.520	−0.535	2304+042	176± 48	−0.133	−2.018
1114+445	55.0± 4.1	0.669	−0.927	1415+451	57.3± 3.9	0.399	−0.579	2308+098	81.5± 6.8	1.616	−0.936

[a] In units of Å. EW values with a decimal point are based on *HST* spectra, while the integer rounded values are based on *IUE* spectra.
[b] In units of $\log(\nu L_\nu/10^{44})$, where νL_ν is measured in erg s^{-1} at rest frame 3000Å.
[c] Log $L/L_{\rm Edd}$.

correlations, we also present in Table 2 the correlations obtained based only on the 46 objects with the generally higher S/N *HST* spectra. The correlations for the *HST* sample are similar, which suggests that the C IV EW measurement uncertainty is not a major source error.

The strongest correlations of the C IV EW are with α_{ox}, and with parameters related to the strength of the [O III] and Fe II lines, and with the Hβ FWHM, which are part of the BG92 EV1 correlations. These correlations confirm earlier results on the inverse relation of the C IV EW and the Fe II strength (Marziani et al. 1996; Wang et al. 1996), the C IV EW EV1 correlations found by Wills et al. (1999, table 1 there) for a smaller sample of 22 BQS quasars (part of our sample), and the earlier results on the C IV EW correlation with α_{ox} (see §1). The correlation with α_{ox} is consistent with the suggestions that the Baldwin effect is driven by a softening of the ionizing continuum (which decreases α_{ox}), with increasing luminosity (Korista et al. 1998). The inverse correlation of the C IV EW and the Fe II strength may be due to optical depth effects. A large optical depth in the Fe II emitting region strengthens the optical Fe II emission by converting UV Fe II emission to optical Fe II emission (Netzer & Wills 1983, Shang et al. 2003). In contrast, a large optical depth in the C IV emitting region results in collisional suppresses of this line (Ferland et al. 1992). Thus, the observed inverse correlation could be produced if the optical depths of the Fe II and C IV emitting regions are related.

Objects with $\alpha_{ox} < -2$, or 'Soft X-Ray Weak' AGN, generally show intrinsic broad C IV absorption (Brandt et al. 2000), whose strength is correlated with luminosity (Laor & Brandt 2002). Incomplete correction for this absorption may induce the observed trend of decreasing C IV EW with decreasing α_{ox}. To avoid absorption biases, we repeated the C IV EW vs. α_{ox} correlation excluding the 12 objects with $\alpha_{ox} < -1.75$ where there is potentially significant absorption. This gave essentially the same result ($r_S = 0.498$, vs. $r_S = 0.525$ for the complete sample), indicating there is no significant absorption bias.

The interesting new result in Table 2 (Fig. 1, middle panel) is the strong correlation of the C IV EW with the $L/L_{\rm Edd}$ indicator (i.e. $L^{1/2}({\rm H}\beta\ {\rm FWHM})^{-2}$), where $r_S = -0.581$ (null probability of Pr $= 1.3\times10^{-8}$). This is not a simple consequence of the separate correlations of the C IV EW with L and with the Hβ FWHM, as for example, the correlation with $M_{\rm BH}$ (i.e. $L^{1/2}({\rm H}\beta\ {\rm FWHM})^{2}$) is insignificant ($r_S = 0.21$, Pr $= 0.05$). However, does the combination of L and Hb FWHM in the form $L^{1/2}({\rm H}\beta\ {\rm FWHM})^{-2}$ produces the tightest correlation? To answer that we searched for the largest r_S in a correlation of log C IV EW with the linear combination $\log L + a\log({\rm H}\beta\ {\rm FWHM})$, where a is a free parameter. We found a maximum correlation of $r_S = -0.588$ at $a = -5.3$, close to the combination of L and Hβ FWHM which provides $L/L_{\rm Edd}$ ($a = -4$). Thus, $L/L_{\rm Edd}$ may be the primary parameter which drives the

Baldwin effect for C IV. This implies that the large scatter in the Baldwin effect is produced by the range of $L/L_{\rm Edd}$ at a given L, as suggested by Shang et al. (2003). However, our results disagree with the suggestion of Shang et al. that the C IV EW is primarily dependent on L, rather than $L/L_{\rm Edd}$.

Is $L/L_{\rm Edd}$ the *only* parameter which controls the C IV EW? Since the EV1 correlations also appear to be driven by $L/L_{\rm Edd}$ (BG92; Boroson 2002), their correlation with the C IV EW could be interpreted as secondary correlations. This can be tested with a partial correlation analysis, which yields an average $r_S = 0.42$ for the correlation of C IV EW with α_{ox} and the EV1 parameters, keeping $L/L_{\rm Edd}$ fixed, and also for the correlation of C IV EW with $L/L_{\rm Edd}$, keeping EV1 and α_{ox} fixed. Although these correlations are weaker than the original ones (Table 2), they are still significant (Pr $\sim 10^{-4}$). The significance of the partial correlations suggests there is a true scatter in the BLR properties at a fixed $L/L_{\rm Edd}$, though it may also be induced by the inaccuracy of our $L/L_{\rm Edd}$ indicator.

The significance of the partial correlations implies that the scatter in the C IV EW vs. $L/L_{\rm Edd}$ relation can be reduced by including a third parameter (in addition to L and the Hβ FWHM, which form $L/L_{\rm Edd}$). The parameter which most significantly improves this correlation is the [O III] λ5007 EW (Fig. 1, lower panel), which yields $r_s = -0.722$ (using $\alpha_{\rm ox}$ instead of [O III] λ5007 EW as a third parameter yields $r_s = -0.667$, and using the Fe II/Hβ flux ratio yields $r_s = -0.674$). Similarly, the most significant fourth parameter is $\alpha_{\rm ox}$ (i.e. correlating log C IV EW vs. a linear combination of log $L/L_{\rm Edd}$, log [O III] λ5007 EW, and $\alpha_{\rm ox}$), which yields a small improvement to $r_s = -0.753$. Finally, the inclusion of the Fe II/Hβ flux ratio as a fifth parameter yields a slight improvement to $r_s = -0.767$.

Some of the scatter in the C IV EW correlations may be induced by a spread in the BLR covering factors among AGN. A plausible way to overcome such a spread is to use the C IV EW/Hβ EW ratio in the above correlations, instead of the C IV EW. This yields significantly *lower* correlations (e.g. the correlations with $L/L_{\rm Edd}$ and $\alpha_{\rm ox}$ go down to -0.391 and 0.391 from -0.581 and 0.525, respectively). This may suggest that the Hβ EW is not a good indicator of the BLR covering factor, but is rather modulated by other BLR properties which do not modulate the C IV EW.

4 CONCLUSIONS

The purpose of this paper is to obtain some indications for the physical parameters which drive the Baldwin effect in C IV through correlation analysis. We use archival *HST* and *IUE* C IV spectra of sufficient quality available for 81 of the 87 BQS quasars, together with the optical emission line parameters from BG92, and $\alpha_{\rm ox}$ from Brandt et al. (2000).

We find that a major source of scatter in the Baldwin effect is the Hβ FWHM. Its inclusion as a second parameter to L, in the form $L^{1/2}\times$(Hβ FWHM)$^{-2}$, which is proportional to $L/L_{\rm Edd}$, leads to a significant increase in the correlation strength (from $r_s = -0.154$ to $r_s = -0.581$). This indicates that the Baldwin effect is a secondary relation, which is induced by the stronger relation of the C IV EW and $L/L_{\rm Edd}$, and the tendency of high L AGN to have a higher $L/L_{\rm Edd}$. This also explains why NLS1s, which are high $L/L_{\rm Edd}$ AGN

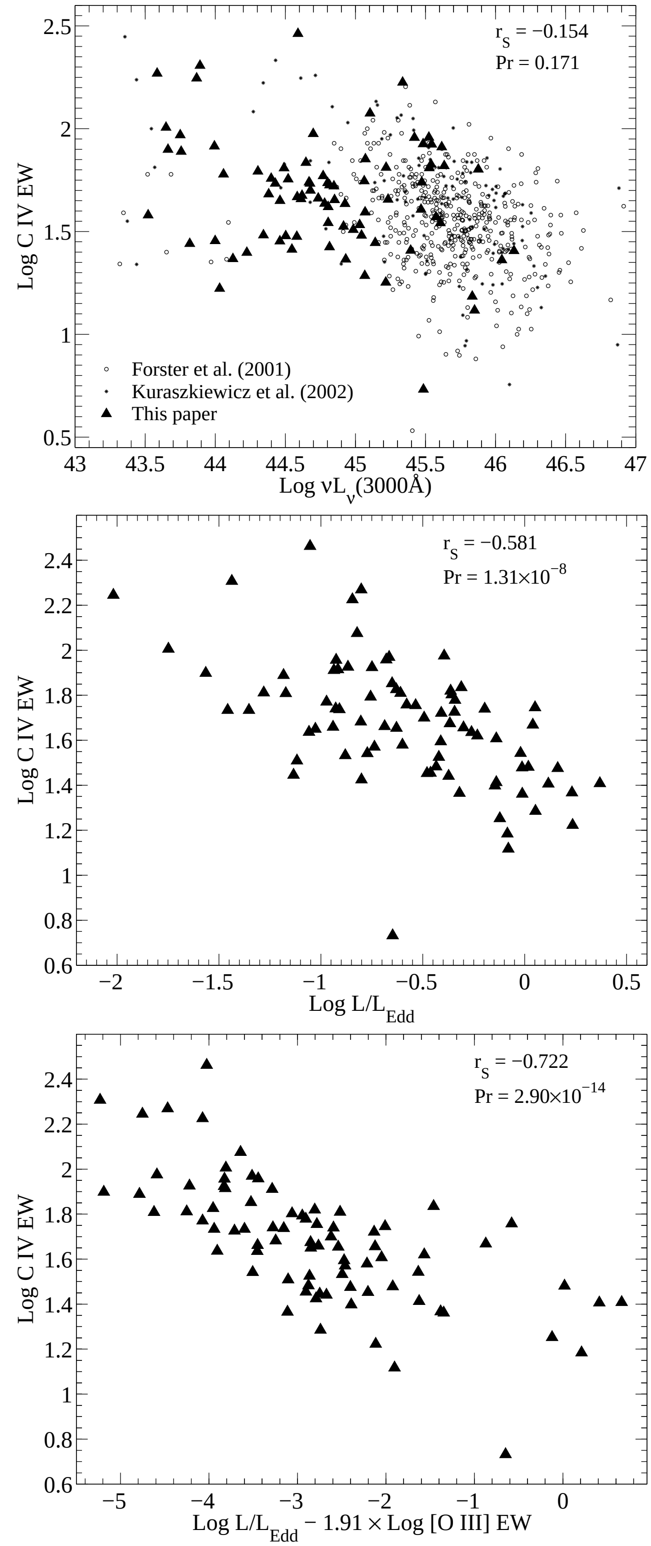

Figure 1. The main C IV EW correlations discussed in this paper. The Spearman rank-order correlation coefficient (r_S) and the null probability (Pr) are indicated at each panel. Top panel: The Baldwin effect for the 81 BQS quasars, together with the Forster et al. (2001) and Kuraszkiewicz et al. (2002) samples. All samples are similarly distributed. Middle panel: The correlation of the C IV EW with $L/L_{\rm Edd}$. Note the significant increase in r_S. Lower panel: The correlation with the addition of [O III] EW as a third parameter, which further increases r_S.

Table 2. The main C IV EW correlations.

Variable Name[a]	r_s[b]	Pr[b]
νL_ν(3000Å)	−0.154	1.71×10^{-01}
	−0.018	9.08×10^{-01}
$L/L_{\rm Edd}$	−0.581	1.31×10^{-08}
	−0.642	1.53×10^{-06}
$\alpha_{\rm ox}$	0.525	4.87×10^{-07}
	0.463	1.18×10^{-03}
[O III] λ5007 EW	0.624	4.71×10^{-10}
	0.708	3.67×10^{-08}
Fe II EW	−0.518	7.49×10^{-07}
	−0.536	1.24×10^{-04}
Hβ FWHM	0.427	7.03×10^{-05}
	0.510	2.92×10^{-04}
R [O III] λ5007 peak height	0.624	4.78×10^{-10}
	0.647	1.20×10^{-06}
R Fe II EW	−0.626	4.02×10^{-10}
	−0.698	6.94×10^{-08}
R [O III] λ5007 EW	0.471	9.23×10^{-06}
	0.494	4.89×10^{-04}

[a] The prefix 'R' indicates the ratio of the variable to that of Hβ (BG92), e.g. R Fe II EW corresponds to Fe II EW/Hβ EW.
[b] The top value for each variable is obtained for the complete sample of 81 objects, the bottom value corresponds to the subsample of 46 objects with *HST* spectra.

at a low L, have much lower C IV EW than expected for their L (as found by Wilkes et al. 1999).

We do not know the physical mechanism responsible for the reduction in the C IV EW with increasing $L/L_{\rm Edd}$. However, we find that the scatter in the Baldwin effect can be further reduced by including either the [O III] EW, the relative Fe II strength, or $\alpha_{\rm ox}$, as a third parameter. The Fe II strength may be an indicator of the BLR optical depth, and $\alpha_{\rm ox}$ may be an indicator of the ionizing continuum shape, which are known theoretically to affect the C IV EW. The physical mechanism implied by the correlation with the [O III] EW remains to be understood. At least some of the remaining scatter can be produced by a non-isotropic, or a time variable continuum source.

The results presented here can be tested with larger samples of AGN. In particular, it will be interesting to explore the extension to high z AGN, where the Hβ region is observable in the IR (e.g. McIntosh et al. 1999; Yuan & Wills, 2003; Shemmer et al. 2004). In addition, different lines show different slopes for the Baldwin effect, and it will be interesting to explore what are the primary physical parameters which drive other emission lines.

ACKNOWLEDGMENTS

We thank the referee for some very helpful remarks. This research has made use of the NASA/IPAC Extragalactic Database (NED), which is operated by the Jet Propulsion Laboratory, California Institute of Technology, under contract with the National Aeronautics and Space Administration.

REFERENCES

Baldwin, J. A., 1977, ApJ, 214, 679
Boroson, T. A., 2002, ApJ, 565, 78
Boroson, T. A., Persson, S. E., & Oke, J. B., 1985, ApJ, 293, 120
Boroson, A. T., & Green, R. F., 1992, ApJS, 80, 109 (BG92)
Brandt, W. N., Laor, A., & Wills, B. J., 2000, ApJ, 528, 637
Brotherton, M. S. & Francis, P. J., 1999, ASP Conf. Ser. 162: Quasars and Cosmology, 395
Croom, S. M. et al., 2002, MNRAS, 337, 275
Dietrich, M., Hamann, F., Shields, J. C., Constantin, A., Vestergaard, M., Chaffee, F., Foltz, C. B., & Junkkarinen, V. T., 2002, ApJ, 581, 912
Espey, B. & Andreadis, S., 1999, ASP Conf. Ser. 162: Quasars and Cosmology, 351
Ferland, G. J., Peterson, B. M., Horne, K., Welsh, W. F., & Nahar, S. N. 1992, ApJ, 387, 95
Forster, K., Green, P. J., Aldcroft, T. L., Vestergaard, M., Foltz, C. B., & Hewett, P. C., 2001, ApJS, 134, 35
Green, P. J., 1998, ApJ, 498, 170
Green, P. J., Forster, K., & Kuraszkiewicz, J., 2001, ApJ, 556, 727
Korista, K., Baldwin, J., & Ferland, G., 1998, ApJ, 507, 24
Kuraszkiewich, J. K., Green, P. J., Forster, K., Aldcroft, T. L., Evans, I. N., & Koratkar, A., 2002, ApJS, 143, 257
Laor, A., 1998, ApJ, 505, L83
Laor, A., 2000, New Astronomy Review, 44, 503
Laor, A., & Brandt, W. N., 2002, ApJ, 569, 641
Laor, A., Banhcall, J. N., Jannuzi, B. T., Schneider, D. P., Green, R. F., & Hatrig, G. F., 1994, ApJ, 420, 110
Marziani, P., Sulentic, J. W., Dultzin-Hacyan, D., Calvani, M., & Moles, M., 1996, ApJS, 104, 37
McIntosh, D. H., Rieke, M. J., Rix, H.-W., Foltz, C. B., & Weymann, R. J., 1999, ApJ, 514, 40
Netzer, H., 1987, MNRAS, 225, 55
Netzer, H. & Wills, B. J., 1983, ApJ, 275, 445
Netzer, H., Laor, A., & Gondhalekar, P. M., 1992, MNRAS, 254, 15
Neugebauer, G., Green, R. F., Matthews, K., Schmidt, M., Soifer, B. T., & Bennett, J., 1987, ApJS, 63, 615
Osmer, P. S. & Shields, J. C., 1999, ASP Conf. Ser. 162: Quasars and Cosmology, 235
Pogge, R. W. & Peterson, B. M., 1992, AJ, 103, 1084
Schlegel, D. J., Finkbeiner, D. P., & Davis, M., 1998, ApJ, 500, 525
Schmidt, M. & Green, R. F., 1983, ApJ, 269, 352
Seaton, M. J., 1979, MNRAS, 187, 73P
Shang, Z., Wills, B. J., Robinson, E. L., Wills, D., Laor, A., Xie, B., & Yuan, J., 2003, ApJ, 586, 52
Shemmer, O., Netzer, H., Maiolino, R., Oliva, E., Croom, S., & Corbett, E., 2004, ASP Conf. Ser.: AGN Physics with the Sloan Digital Sky Survey, 407
Wang, T., Zhou, Y., & Gao, A., 1996, ApJ, 457, 111
Wilkes, B. J., Kuraszkiewicz, J., Green, P. J., Mathur, S., & McDowell, J. C., 1999, ApJ, 513, 76
Wills, B. J., Laor, A., Brotherton, M. S., Wills, D., Wilkes, B. J., Ferland, G. J., & Shang, Z., 1999, ApJ, 515, L53
Yuan, M. J. & Wills, B. J., 2003, ApJ, 593, L11